

Physically-Plausible Modelling of Biomolecular Systems: A Simplified, Energy-Based Model of the Mitochondrial Electron Transport Chain

Peter J. Gawthrop^{1,a,b}, Peter Cudmore^{a,c}, Edmund J. Crampin^{a,b,c}

^a*Systems Biology Laboratory, Department of Biomedical Engineering, Melbourne School of Engineering, University of Melbourne, Victoria 3010, Australia*

^b*Systems Biology Laboratory, School of Mathematics and Statistics, University of Melbourne, Victoria 3010, Australia*

^c*ARC Centre of Excellence in Convergent Bio-Nano Science and Technology, School of Chemical and Biomedical Engineering, Melbourne School of Engineering, University of Melbourne, Victoria 3010, Australia*

Abstract

Advances in systems biology and whole-cell modelling demand increasingly comprehensive mathematical models of cellular biochemistry. Such models require the development of simplified representations of specific processes which capture essential biophysical features but without unnecessarily complexity. Recently there has been renewed interest in thermodynamically-based modelling of cellular processes. Here we present an approach to developing of simplified yet thermodynamically consistent (hence physically plausible) models which can readily be incorporated into large scale biochemical descriptions but which do not require full mechanistic detail of the underlying processes. We illustrate the approach through development of a simplified, physically plausible model of the mitochondrial electron transport chain and show that the simplified model behaves like the full system.

1. Introduction

In mathematical biology, and more widely, the relative merits of simple ‘toy’ models, which represent some key aspects of the system but not full mechanistic detail, and comprehensive mechanistically detailed representations have long been debated.

¹Corresponding author. peter.gawthrop@unimelb.edu.au

Simple ‘toy’ models allow rigorous mathematical analysis and are generally easy to simulate, but are difficult to relate to the full system and measurements thereof. Full mechanistically detailed models on the other hand provide a straight-forward mapping to the real system, but are challenging to parameterize and analyse, and may require significant computational overhead to simulate.

Simple models of complex biochemical processes can elucidate basic behaviour and biologically significant trade-offs (Scott et al., 2014; Weiße et al., 2015) and as such can be used as an aid to synthetic biology (Darlington et al., 2018). Furthermore, models of individual processes may be used as part of a model of an overall system as, for example, in the Physiome Project (Crampin et al., 2004; Hunter, 2016), or in whole-cell modelling (Karr et al. (2012); Macklin et al. (2014); this requires models to be modular and reusable (Neal et al., 2014; Nickerson et al., 2016).

Recently there has been renewed interest in thermodynamically-based mechanistic modelling of cellular processes (Mason and Covert, 2019; Pan et al., 2019; Gawthrop et al., 2017; Klipp et al., 2016; Beard and Qian, 2010). A modular approach to energy-based modelling has been developed in the context of biomolecular systems (Gawthrop et al., 2015; Gawthrop and Crampin, 2016). This raises the question as to whether it is possible to develop energy-based models that are nevertheless simple.

Like engineering systems, living systems are subject to the laws of physics in general and the laws of thermodynamics in particular. This fact gives the opportunity of applying engineering approaches to the modelling, analysis and understanding of living systems. The bond graph method of Paynter (1961) is one such well-established engineering approach (Cellier, 1991; Gawthrop and Smith, 1996; Gawthrop and Bevan, 2007; Borutzky, 2010; Karnopp et al., 2012) which has been extended to include biomolecular systems (Oster et al., 1971, 1973; Gawthrop and Crampin, 2014, 2017; Gawthrop et al., 2017; Gawthrop and Crampin, 2018a,b; Pan et al., 2018, 2019).

When developing simplified models of biomolecular systems where energy transduction is important, it is essential that models be *physically-plausible*. A *physically-plausible* model of a physical system has two attributes: it is itself a model of a physical system (i.e. it does not contravene the laws of physics); and it shares key behaviours with the actual physical system (Gawthrop, 2003). Such an approach will, however,

only be of use if there are complex physical systems which can indeed be represented by a simpler physical model. This paper shows that this is indeed the case. In particular we demonstrate that it is possible to develop a simplified model of the mitochondrial electron transport chain that is thermodynamically consistent, but which doesn't represent full mechanistic detail, and show that it behaves like the full model.

Mitochondria make use of reduction-oxidation (redox) reactions in which the transfer of electrons is used to provide the power driving many living systems. As discovered by Mitchell (1961, 1976, 1993, 2011), the key feature of mitochondria is the *chemiosmotic* energy transduction whereby a chain of redox reactions pumps protons across the mitochondrial inner membrane to generate an electrochemical gradient known as the *proton-motive force* (PMF). The PMF is then used to power the synthesis of ATP – the universal fuel of living systems. Due to this central role in living systems, mathematical modelling of the key components of mitochondria is thus an important challenge to systems biology. Because mitochondria transduce energy, an energy-based modelling method is desirable, and Beard and colleagues have developed the most comprehensive such models to date (Beard, 2005; Wu et al., 2007; Beard and Qian, 2010; Beard, 2012; Bazil et al., 2016). A bond graph model of mitochondrial oxidative phosphorylation has been given by Gawthrop (2017). This model is based on modelling the redox reactions associated with complexes CI, CIII and CIV of the mitochondrial electron transport chain.

Below we briefly outline the bond graph approach to modelling energy flows in biochemical reactions, in particular describing the Faraday-equivalent potential approach to modelling electrochemical phenomena, and we describe a modified mass action kinetics approach which will be central to development of a simplified thermodynamic modelling approach. A set of Python based tools has been developed to assist the development and analysis of bond graph models and these tools are briefly outlined.

We then discuss the Mitochondrial Electron Transport Chain (ETC) as an example of a complex biomolecular system which can be successfully modelled by a simple physically-plausible model, and use data from Bazil et al. (2016) to derive parameters of the physically-plausible of the ETC to show that this simple model behaves the same as a fully mechanistic description of the ETC. Finally we conclude with suggestions for

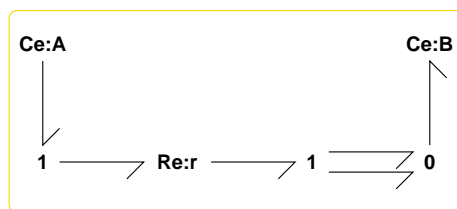


Figure 1: Bond Graph representation of $A \xrightleftharpoons{r} 2B$. The bond graph components **Ce:A** and **Ce:B** represent species A and B; the bond graph component **Re:r** represents the reaction the bonds \rightarrow together with the zero **0** and one **1** junctions define the stoichiometry (Gawthrop and Crampin, 2014). The bonds carry the energy covariables chemical potential μ and molar flow v .

future research directions using simplified physically-plausible modelling as a strategy in systems and synthetic biology.

2. Modelling Bioenergetics of Biochemical Systems using Bond Graphs

Bond graphs provide a convenient modular framework for modelling energy flow within and across different physical domains: electrical, mechanical, chemical and so on; and as such are useful for representing biomolecular systems. In brief, bonds represent pairs of variables: potential and flow, whose product is power. In the biomolecular domain, the product of chemical potential μ (with units J mol^{-1}) and molar flow v (with units mol s^{-1}) is power with units J s^{-1} (Oster et al., 1971, 1973; Gawthrop and Crampin, 2014). Bonds connect components which represent either storage or dissipation of energy. In biomolecular systems, chemical potential is stored as concentration of chemical species, denoted **Ce**², whereas chemical reactions, denoted **Re**, in which chemical species are converted from one form to another are dissipative processes. The biochemical network stoichiometry is represented in the coupling of **Ce** components via the reactions **Re** using bonds which represent the flow of energy, connected using common potential **0** ('zero') and common flow **1** ('one') junctions.

²In this paper, **Ce** components are used to represent chemical species and **C** components to represent electrical capacitors.

To illustrate, Figure 1 is the bond graph representation of the chemical reaction:



Ce components correspond to constitutive relations which relate the chemical potential to the amount of chemical species stored: the constitutive relations of **Ce:A** and **Ce:B** are:

$$\mu_A = RT \ln K_A x_A \quad (2.2)$$

$$\mu_B = RT \ln K_B x_B \quad (2.3)$$

where x_A and x_B are the concentrations of A and B, K_A and K_B are species thermodynamic constants (mol^{-1}) for A and B, specific to each chemical species, R is the universal gas constant and T the absolute temperature.

The constitutive relations for the reaction components **Re** provide the relationship between forward and backward chemical affinities A (stoichiometric combinations of the chemical potentials) which provide the driving force for the reaction, and the molar flow (the reaction rate) f . The stoichiometry of reaction **Re:r** with formation of 2 molecules of species B for each molecule of A is represented by the two parallel bonds on the right hand side of **Re:r**. With mass-action kinetics, the constitutive relation of **Re:r** is

$$f = \kappa \left(\exp \frac{A^f}{RT} - \exp \frac{A^r}{RT} \right) \quad (2.4)$$

where κ is a reaction rate constant (mol s^{-1}), specific to each reaction, and the forwards and backwards affinities are given by

$$A^f = \mu_A \quad (2.5)$$

$$\text{and } A^r = 2\mu_B \quad (2.6)$$

Combining these expressions gives the familiar mass-action expression for the reaction flow f :

$$f = \kappa \left(K_A x_A - K_B^2 x_B^2 \right) \quad (2.7)$$

where the forward reaction rate constant $k^+ = \kappa K_A$ and the reverse reaction rate constant $k^- = \kappa K_B^2$.

The bond graph approach is naturally allied to stoichiometric concepts (Klipp et al., 2016; Palsson, 2006, 2011, 2015). In particular, the stoichiometric matrix N can be automatically generated from the network represented in the system bond graph. N can be used to give species flows f_x in terms of reaction flows f and, conversely, reaction affinity A in terms of species potentials μ :

$$f_x = Nf \qquad A = -N^T\mu \qquad (2.8)$$

In the case of the system of Figure 1:

$$N = \begin{pmatrix} -1 & 2 \end{pmatrix}^T \qquad (2.9)$$

2.1. Modified mass action kinetics

Simplified representation of biomolecular system requires a representation of the reaction network that approximates, but does not fully represent the complete set of biochemical reactions. Physically-plausible models of biomolecular systems will therefore typically contain reactions which are an approximation to a sequence of elementary reactions. Thus even if elementary reaction steps have the mass action kinetics of Equation (2.4), this would not necessarily be the case for the overall reactions used to represent the system (see for example Atkins et al., 2018, chapter 17).

In bond graph terms, one may represent the dissipative reaction component with any appropriate constitutive relation for the reaction flow f in terms of the forward and reverse affinities: mass action, as given by (2.4) leading to (2.7) is one example. In particular, non-elementary reactions may be represented using rate equations where, unlike the mass-action formulation, the concentration exponents are not the stoichiometric coefficients. One particular case of this would be to divide all of the stoichiometric coefficients by an positive integer constant α in the rate equations. Thus, for example, if $\alpha = 2$, the reaction rate (2.7) corresponding to the reaction (2.1) would become:

$$f = \kappa \left(\sqrt{K_A x_A} - K_B x_B \right) \qquad (2.10)$$

This corresponds to the non-integer stoichiometry

$$N_\alpha = \begin{pmatrix} -\frac{1}{2} & 1 \end{pmatrix}^T \qquad (2.11)$$

Note that in the context of modelling the Mitochondrial Electron Transport Chain, the exponent $1/2$, corresponding to $\alpha = 2$, commonly appears in the flux expression for complex III, as given by Beard (2005, equation B72) and Beard and Qian (2010, equation 7.38) for example, and the exponent $1/4$, corresponding to $\alpha = 4$, appears in the flux expression for complex IV given by Beard (2005, equation B73) and Beard and Qian (2010, equation 7.41). This can be achieved by replacing the mass-action formula (2.4) by the *modified mass-action* (MMA) formula:

$$f = \kappa \left(\exp \frac{A^f}{\alpha RT} - \exp \frac{A^r}{\alpha RT} \right) \quad (2.12)$$

which contains the additional parameter α , which is used below as an essential part of the model fitting process.

For thermodynamic consistency, it is important that Equation (2.12) represents a dissipative system; that is, any non zero flow dissipates energy (Willems, 1972; Polderman and Willems, 1997; Willems, 2007). With this in mind, it is now shown that the MMA equation can be rewritten in mass-action form but with the positive *constant* κ replaced by the positive *function* of concentration κ_α . As a simple example of this, it can be verified that Equation (2.10) can be rewritten as

$$f = \kappa_\alpha (K_A x_A - K_B^2 x_B^2) \quad (2.13)$$

$$\text{where } \kappa_\alpha(x_A, x_B) = \frac{\bar{\kappa}}{\sqrt{K_A x_A + K_B x_B}} \quad (2.14)$$

As x_A and x_B are positive, κ_α is also positive. Thus (2.13) corresponds to the mass-action equation (2.4) with the positive constant κ replaced by the positive function of concentration $\kappa_\alpha(x_A, x_B)$. The general modified-mass action kinetics of Equation (2.12) can also be rewritten in mass-action form with the positive constant κ replaced by the positive κ_α :

$$f = \kappa_\alpha(A^f, A^r) \left(\exp \frac{A^f}{RT} - \exp \frac{A^r}{RT} \right) \quad (2.15)$$

2.2. Redox reactions

Oxidative phosphorylation involves a series of electrochemical redox reactions. Nicholls and Ferguson write that ‘Whereas all redox reactions can quite properly be

described in thermodynamic terms by their Gibbs energy changes, electrochemical parameters can be employed because the reactions involve the transfer of electrons.” (Nicholls and Ferguson, 2013, chapter 3.3). Rather than to deal directly with conversion between electrical and chemical potentials and associated variables, it is convenient to have a common system of units and convert the chemical energy covariables chemical potential and molar flow to equivalent electrical energy covariables voltage and current (Gawthrop, 2017). The relevant conversion factor is *Faraday’s constant* $F \approx 96\,485 \text{ C mol}^{-1}$ (Nicholls and Ferguson, 2013; Gawthrop et al., 2017; Gawthrop, 2017). In particular, we define:

$$\text{Faraday-equivalent potential} \quad \phi = \frac{\mu}{F} \text{ (V)} \quad (2.16)$$

$$\text{Faraday-equivalent flow} \quad f = Fv \text{ (A)} \quad (2.17)$$

Using these Faraday-equivalent variables, the **Ce** constitutive relations (2.2) and (2.3) become:

$$\phi_A = V_N \ln K_A x_A \quad (2.18)$$

$$\phi_B = V_N \ln K_B x_B \quad (2.19)$$

$$\text{where } V_N = \frac{RT}{F} \approx 26 \text{ mV} \quad (2.20)$$

and the modified mass-action formula (2.12) becomes:

$$f = \kappa \left(\exp \frac{A^f}{\alpha V_N} - \exp \frac{A^r}{\alpha V_N} \right) \quad (2.21)$$

As noted by Nicholls and Ferguson, an advantage of transforming the chemical potentials into equivalent electrical potentials in the treatment of redox reactions is: “the ability to dissect the overall electron transfer into two half-reactions involving the donation and acceptance of electrons, respectively.” (Nicholls and Ferguson, 2013, chapter 3.3). For example, the two half-reactions:



electron e_1^- donation in the first (oxidation of A), and e_2^- acceptance in the second (reduction of B), correspond to the overall reaction:



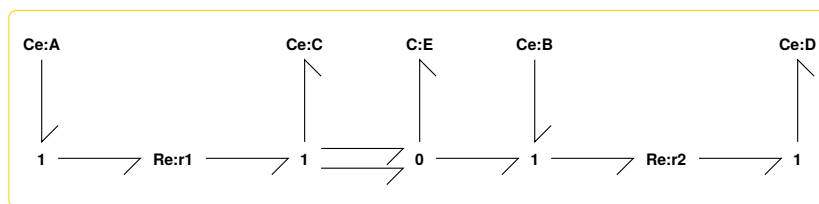


Figure 2: Bond Graph representation of two half-reactions: $A \xrightleftharpoons{r_1} C + 2e^-$ and $B + e^- \xrightleftharpoons{r_2} D$. As in Figure 1, the bond graph components **Ce:A**, **Ce:B**, **Ce:C** and **Ce:D** represent species A, B, C and D; the bond graph component **Re:r1** represent the two half-reactions; the bonds \rightarrow together with the zero **0** and one **1** junctions define the stoichiometry. The component **C:E** represents the electrons of the half-reaction and is related to the redox potentials. The corresponding voltage is V . As discussed in § 2.2, the bonds carry the energy covariables electrical potential ϕ and and current v .

Figure 2 shows a bond graph representation of these two half-reactions (2.22), explicitly representing the transfer of electrons e^- using the linear electrical capacitor represented by **C:E** with voltage V ; the two-electron stoichiometry of reaction r_1 is represented by the two parallel bonds. If reaction r_1 is in equilibrium, then the voltage V is exactly that required to stop reaction r_1 from proceeding and thus $V = -E_1$ where E_1 is the *redox potential* of reaction r_1 . Conversely, if reaction r_2 is in equilibrium, then the voltage V is exactly that require to stop reaction r_2 from proceeding and thus $V = -E_2$ where E_2 is the *redox potential* of reaction r_2 .

2.3. Hierarchical Modelling

Hierarchical modelling and modularity provide one approach to understanding the complex systems associated with cellular biochemistry (Hartwell et al., 1999; Lauffenburger, 2000; Csete and Doyle, 2002; Bruggeman et al., 2002, 2008; Szallasi et al., 2010). Bond graphs provide an effective foundation for modular construction of hierarchical models of biochemical systems (Gawthrop et al., 2015; Gawthrop and Crampin, 2016). Bond graphs model the interaction between modules, in particular retroactivity (Jayanthi and Del Vecchio, 2011; Del Vecchio, 2013; Del Vecchio and Murray, 2014), in a straightforward manner whilst retaining thermodynamic compliance.

Bond graph modules use the notion of *chemostats* (Poletti and Esposito, 2014; Gawthrop and Crampin, 2016) which have an number of interpretations:

1. one or more species is fixed to give a constant concentration; this implies that an appropriate external flow is applied to balance the internal flow of the species.
2. as a **Ce** component with a fixed state.
3. as a module *port* through which chemical, mechanical or electrical energy flows.

Thus if the bond graph of Figure 2 were to be used as a module, then **Ce:A**, **Ce:B**, **Ce:C** and **Ce:D** could be chemostats. If the module were to be examined in isolation, then the interpretations of items 1 and 2 would be used; if, on the other hand, the module were to be embedded in a larger system, then the interpretation of item 3 would be used.

When examining the properties of a complex system, such as a whole cell model, the replacement of some modules by physically-plausible equivalents with the same ports would not only reduce computational complexity but also allow attention to be focussed on detailed models of other modules.

2.4. Dynamical Simulation

Bond graphs, together with the component constitutive relationships, can be used to automatically derive the ordinary differential equations (ODE) describing the system dynamics (Karnopp et al., 2012). These ODEs can be in symbolic form or in the form of computer code for a particular simulation engine. In general, a set of ODEs does not guarantee thermodynamic consistency; but, because these ODEs are derived from a bond graph, they inherit the thermodynamic properties of the bond graph.

In some systems, the system states are not independent; in particular, biomolecular systems usually have conserved moieties. In such circumstances, the system bond graph can be used to automatically generate the minimal number of ODEs describing the independent states from which dependent states and reaction flows can be derived (Gawthrop and Crampin, 2014, § 3(c)).

Although in this paper we have focused on species described by the standard logarithmic constitutive relation (2.2) and reaction flows determined by the mass action formula (2.4), bond graph components can have a wide range of constitutive relations constrained only by thermodynamics. A simple example of this is the modified mass-action formula of equation (2.12); a more complex example is the Goldman-Hodgkin-

Katz flux equation used in bond graph models of action potential (Gawthrop et al., 2017). Moreover, models with complex characteristics, such as transporters, can be built from simple bond graph components (Pan et al., 2019).

2.5. *BondGraphTools* – a Python Toolkit

Computational tools are necessary for model capture, parameterisation and simulation. As the name suggests, `BondGraphTools` is an application programming interface (API) for capturing, simplifying and simulating bond graph models, and is an important part of the bond graph approach (Cudmore et al., 2019).

`BondGraphTools` is written in Python and is built upon the Scientific Python (SciPy) libraries, all of which are open source and easily accessible. The core use-case of `BondGraphTools` is to turn bond graphs into a set of reduced equations which can be then passed into other SciPy libraries (parameter estimation routines, or ODE integrators, for example). As model reduction is performed symbolically, the simplification routines are free from numerical errors, which is important for systems involving parameters that are unknown.

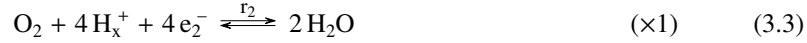
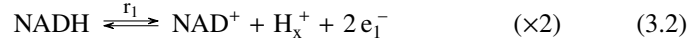
3. A Simplified Physically-Plausible Model for the Mitochondrial Electron Transport Chain

Mitochondria make use of redox reactions to provide the power driving many living systems. The key process in the generation of ATP is *chemiosmotic* energy transduction, whereby a sequence of redox reactions pumps protons across the mitochondrial inner membrane to generate the *proton-motive force* (PMF), an electrochemical gradient which is then used to power the synthesis of ATP. Generation of the PMF is accomplished by the mitochondrial electron transport chain. Beard and colleagues have developed the most comprehensive thermodynamically consistent models of mitochondrial oxidative phosphorylation including the electron transport chain (Beard, 2005; Wu et al., 2007; Bazil et al., 2016). Recently Gawthrop (2017) provided a bond graph model of mitochondrial oxidative phosphorylation based on the redox reactions associated with complexes CI, CIII and CIV of the mitochondrial electron transport chain.

In contrast, here we develop a simple, but physically-plausible, model based on the overall chemical reaction of the Electron Transport Chain in which 2 NADH is combined with O_2 and $2 H^+$ to give $2 NAD^+$ and $2 H_2O$; the 2 protons ($2 H^+$) are consumed from the mitochondrial matrix. The free energy of this overall reaction pumps 20 protons across the mitochondrial inner membrane. Denoting the protons in the mitochondrial matrix as H_x^+ and those in the mitochondrial inner membrane space as H_i^+ the overall reaction is thus:



Reaction (3.1) can be rewritten as the weighted sum of three reactions:



where e_1^- and e_2^- are the electrons transferred from and to the left and right half reactions respectively as discussed in § 2.2. Reaction (3.2) converts NADH to NAD producing a proton H_x^+ in the mitochondrial matrix and *donating* two electrons e_1^- . Reaction (3.3) converts O_2 and protons H_x^+ in the mitochondrial matrix and *consumes* four electrons e_2^- to produce water H_2O . Reaction (3.4) *transfers* electrons e_1^- to e_2^- and, in so doing, utilises the corresponding free energy to pump five protons from the mitochondrial matrix H_x^+ to the mitochondrial inter-membrane space H_i^+ against the H^+ concentration gradient and the trans-membrane electrical potential $\Delta\Psi$.

Figure 3 shows the bond graph of a physically-plausible model of the mitochondrial electron transport chain. The the components of the model are:

1. The electron donation reaction r_1 (3.2) is represented by **Re:r1** and the associated species by **Ce:NADH**, **Ce:NAD** and **Ce:Hx**. The electrons e_1^- accumulate in the electrical capacitor **C:E1**.
2. The electron consumption reaction r_2 (3.3) is represented by **Re:r2** and the associated species by **Ce:O2**, **Ce:H2O** and **Ce:Hx**. The electrons e_2^- accumulate in the electrical capacitor **C:E2**.

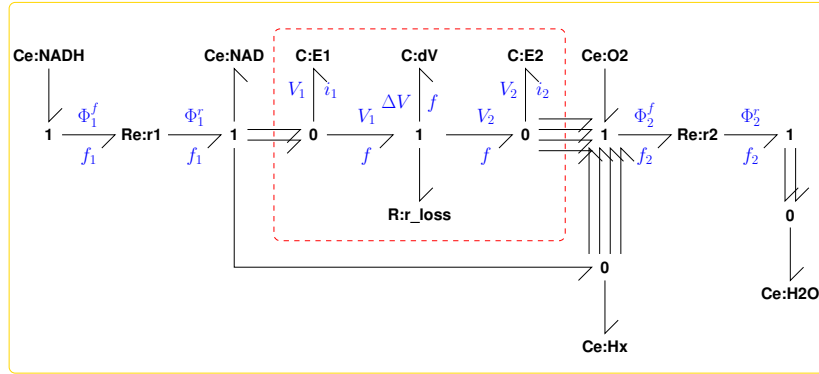


Figure 3: Mitochondrial electron transport chain: a physically-plausible model. The reaction represented by **Re:r1** is the electron donating reaction (3.2) and the reaction represented by **Re:r2** is the electron consuming reaction (3.3). The dashed box demarcates the electrical part of the model: the electrical resistor **R:r_loss** models electrical energy dissipation; **C:E1** and **C:E2** are electrical capacitors accumulating donated and consumed electrons. The electrical capacitor **C:dV** corresponds to the net voltage available to pump protons across the mitochondrial inner membrane.

3. The electron transfer part of the electron transfer/proton pump (3.4) is modelled by the two electrical capacitors **C:E1** and **C:E2** and the (linear) electrical resistor (with resistance r_{loss}) **R:r_loss**. The voltage V_1 associated with **C:E1** is the redox potential of half reaction (3.2) and the voltage V_2 associated with **C:E2** is the redox potential of half reaction (3.3). The electrical capacitor **C:dV** with voltage ΔV represents by the the net redox potential minus the potential drop associated with the resistor r_{loss} :

$$\Delta V = V_1 - V_2 - r_{loss}f \quad (3.5)$$

4. Proton transfer is not explicitly modelled in Fig. 3. However, the corresponding membrane potential $\Delta\Psi$ is given in terms of ΔV as by:

$$\Delta\Psi = \frac{\Delta V}{n_p} - \Phi_H \quad (3.6)$$

where $n_p = \frac{20}{4} = 5$ is the number of protons pumped per electron and $\Phi_H = \phi_{Hi} - \phi_{Hx}$, the chemical potential difference due to proton concentration difference across the membrane.

Substance	ρ	ϕ^\ominus (V)	ϕ^\ominus (V)
H ₂ O	1.000	-2.443	-2.443
H _x ⁺	1.660×10^{-8}	0.000	-4.217×10^{-1}
NAD ⁺	1.500×10^{-3}	1.876×10^{-1}	3.454×10^{-2}
NADH	1.500×10^{-3}	4.074×10^{-1}	2.544×10^{-1}
O ₂	2.500×10^{-5}	1.700×10^{-1}	-7.945×10^{-2}

Table 1: Physical Parameters of the Physically-plausible model. x^\ominus is the concentration at nominal conditions relative to standard conditions, ϕ^\ominus and ϕ^\ominus are the Faraday-equivalent potentials at standard and nominal conditions related by Equation (3.8) and where ρ is given by Equation (3.9). H_x⁺ are protons in the matrix.

3.1. Physical Parameters

The **Ce** constitutive relation (2.18) can be rewritten in the alternative form:

$$\phi_A = \phi_A^\ominus + V_N \ln \frac{x_A}{x_A^\ominus} \quad (3.7)$$

where V_N is given by (2.20) and ϕ^\ominus is the potential of substance A at standard conditions where $x_A = x_A^\ominus$. Using tables of standard chemical potentials μ^\ominus , equation (2.16) can be used to derive the corresponding potential ϕ^\ominus . As discussed by Gawthrop (2017), the Faraday-equivalent chemical potential of substance A at nominal conditions ϕ^\ominus can be computed from Faraday-equivalent chemical potential at standard conditions ϕ^\ominus from the formula:

$$\phi_A^\ominus = \phi_A^\ominus + V_N \ln \rho_A \quad (3.8)$$

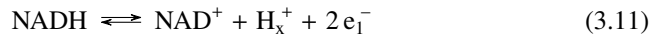
$$\text{where } \rho_A = \frac{x_A^\ominus}{x_A^\ominus} \quad (3.9)$$

where x_A^\ominus and x_A^\ominus are the concentrations of substance A at nominal conditions and standard conditions. Table 1 shows nominal values ϕ^\ominus for a number of different substances. These values will be used below to model the mitochondrial electron transport chain.

The stoichiometric equations (2.8) can be rewritten in Faraday-equivalent form as

$$f_x = Nf \quad \Phi = -N^T \phi \quad (3.10)$$

In the case of the half-reaction (3.2)



the stoichiometric matrix is:

$$N^T = \begin{pmatrix} -1 & 1 & 1 & 2 \end{pmatrix} \quad (3.12)$$

It follows that the reaction potential Φ is:

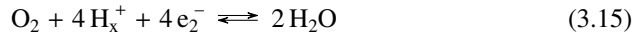
$$\Phi = N^T \phi = \phi_{NADH}^\circ - \phi_{NAD}^\circ - \phi_{Hx}^\circ - 2\phi_E^\circ \quad (3.13)$$

At equilibrium, $\Phi = 0$ and so:

$$\begin{aligned} V = \phi_E^\circ &= \frac{1}{2} (\phi_{NADH}^\circ - \phi_{NAD}^\circ - \phi_{Hx}^\circ) \\ &= \frac{1}{2} (254.4 - 34.54 - (-421.7)) \approx 320 \text{ mV} \end{aligned} \quad (3.14)$$

and so this corresponds to a redox potential of $E = -V = -320 \text{ mV}$ for this half-reaction.

Similarly, in the case of the half-reaction (3.3)



the redox potential is $E = -V = 780 \text{ mV}$.

3.2. An explicit formula

From a systems point of view, the model of the ETC can be characterised by the voltage/current relationship of the bond graph component $\mathbf{C:dV}$. This represents the steady state relationship between the flow (rate of electron transport along the ETC, or equivalently the rate of oxygen consumption) and the mitochondrial membrane potential which is established. Letting n_1 and n_2 be the number of bonds connecting reactions r_1 and r_2 to the electrical subsystem, the steady-state flows are related by:

$$f = n_1 f_1 = n_2 f_2 \quad (3.16)$$

and the steady-state potentials by Equation (3.5) with:

$$V_1 = \frac{1}{n_1} \Phi_1 \quad (3.17)$$

$$\text{and } V_2 = \frac{1}{n_2} \Phi_2 \quad (3.18)$$

Using the modified mass action formula (2.21), the reaction flows are given by

$$f_1 = \kappa_1 \left(\exp \frac{\Phi^f_1}{\alpha V_N} - \exp \frac{\Phi^r_1 + n_1 V_1}{\alpha V_N} \right) \quad (3.19)$$

$$f_2 = \kappa_2 \left(\exp \frac{\Phi^f_2 + n_2 V_2}{\alpha V_N} - \exp \frac{\Phi^r_2}{\alpha V_N} \right) \quad (3.20)$$

where the parameter α remains to be determined (by fitting to data). At equilibrium, the flows are zero and thus:

$$V_1 = V_1^{eq} = \frac{1}{n_1} (\Phi^f_1 - \Phi^r_1) = \frac{1}{n_1} \Phi_1 \quad (3.21)$$

$$V_2 = V_2^{eq} = \frac{1}{n_2} (\Phi^r_2 - \Phi^f_2) = -\frac{1}{n_2} \Phi_2 \quad (3.22)$$

Writing $\Delta V_1 = V_1 - V_1^{eq}$ and $\Delta V_2 = V_2 - V_2^{eq}$ it follows that the flows can be rewritten as:

$$f_1 = (1 - \lambda_1) K_1 \quad f_2 = (\lambda_2 - 1) K_2 \quad (3.23)$$

where

$$\lambda_1 = \exp \frac{n_1 \Delta V_1}{\alpha V_N} \quad \lambda_2 = \exp \frac{n_2 \Delta V_2}{\alpha V_N} \quad (3.24)$$

$$K_1 = \kappa \exp \frac{\Phi^f_1}{\alpha V_N} \quad K_2 = \kappa \exp \frac{\Phi^r_2}{\alpha V_N} \quad (3.25)$$

Hence using (3.23)

$$\lambda_1 = 1 - \frac{f}{n_1 K_1} \quad \lambda_2 = 1 + \frac{f}{n_2 K_2} \quad (3.26)$$

Using (3.24) and (3.5)

$$\Delta V = \Delta V^{eq} + \frac{\alpha V_N}{n_1} \ln \left(1 - \frac{f}{n_1 K_1} \right) - \frac{\alpha V_N}{n_2} \ln \left(1 + \frac{f}{n_2 K_2} \right) - r_{loss} f \quad (3.27)$$

where $\Delta V^{eq} = V_1^{eq} - V_2^{eq}$. Using the results of § 3.1

$$\Delta V^{eq} = 320 + 780 = 1100 \text{ mV} \quad (3.28)$$

This formula, derived from the simplified model using modified mass action, thus provides a voltage/current steady state relationship that describes the operation of the ETC. Using equation (3.6) and a value of $\Phi_H = 25 \text{ mV}$ this corresponds to an equilibrium mitochondrial membrane potential $\Delta \Psi_{eq}$ of: $\Delta \Psi_{eq} = \frac{1100}{5} - 25 = 195 \text{ mV}$.

3.3. Model Fitting

The simplified, physically plausible model of the electron transport chain derived above contains physical parameters which are known *a-priori*, as well as parameters which are model-dependent and must be obtained by fitting to relevant data. In particular, the explicit formula (3.27) relating flow f to potential difference ΔV has four known physical parameters: ΔV^{eq} , V_N , n_1 and n_2 and four unknown parameters: α , K_1 , K_2 and r_{loss} . Bazil et al. (2016) develop a detailed physically based mathematical model of mitochondrial oxidative phosphorylation and ROS generation and compare the results with *in-vitro* experimental data. These results are used below to fit the parameters of the physically-plausible model developed above.

Figure 2B in Bazil et al. shows four datasets: two sets of simulation results corresponding to two concentrations of inorganic phosphate Pi: $[Pi] = 1 \text{ mM}$ and $[Pi] = 5 \text{ mM}$, and two sets of experimental data corresponding to these two conditions. The maximum value for V_{O_2} (Figure 2B in Bazil et al.) is 150 nmol/min/UCS . This value is used to normalise the reported flows for the purposes of parameter fitting. Thus in Figure 5, the mitochondrial membrane potential $\Delta\Psi \text{ mV}$ is plotted against the normalised rate of oxygen consumption f . In ideal circumstances, the experimental data would correspond to an isolated module where the species concentrations corresponding to each chemostat in the model (see § 2.3) were constant. This is not the case here as, for example, NADH is generated from the mitochondrial TCA (citric acid) cycle and so concentration of NADH depends on the flow through the TCA cycle.

For the purposes of illustrating parameter fitting in the context of physically-plausible models, this lack of isolation is not included; but would be an interesting topic of future research.

A further approximation is that inorganic phosphate Pi does not appear in the physically plausible model developed above and therefore it is not possible to take account of the variation of Pi in this approximate model. However, the experimental data shown in Figure 2B of Bazil et al. does not show a strong dependence of this part of the system on Pi and so the lack of dependence of our simplified model on Pi is reasonable. For this reason, experimental data for both values of Pi are considered for the purposes of model fitting to the raw data. We note that other components of

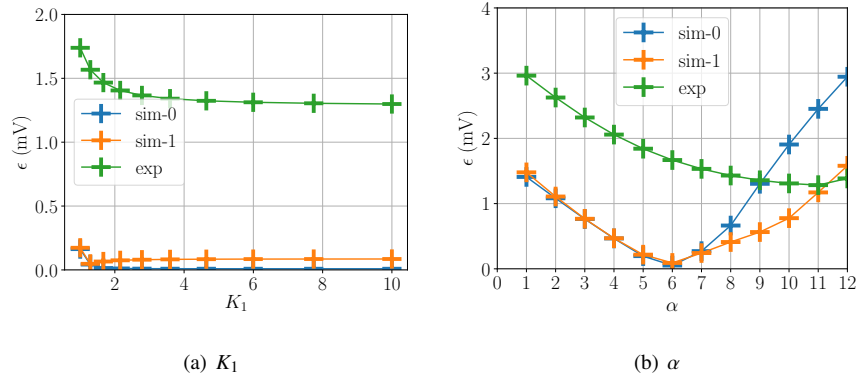


Figure 4: Fitting K_1 and α . (a) The RMS error ϵ as parameter K_1 is varies; all other parameters are optimised. The value of K_1 is not important if greater than about 2; the reaction r1 is in equilibrium. (b) The RMS error ϵ as parameter α of the modified mass-action kinetics (2.21) is varies; all other parameters are optimised. For data sets `sim-0` and `sim-1` (data from the experimentally fitted model of Bazil et al. (2016)) there is a clear minimum at about $\alpha = 6$.

mitochondrial metabolism not modelled here, such as ATPase, do depend strongly on Pi.

Known physical parameters Φ^\ominus of Table 1 are drawn from the supplementary material of Wu et al. (2007), the concentrations of NAD and NADH from Bazil et al. (2016), the pH values from Porcelli et al. (2005) and the O_2 concentration from Murphy (2009). Parameter fitting was implemented using the Python function within the SciPy.optimize module `opt.minimize` with `method = "L-BFGS-B"` and parameter bounds of 10^{-12} and ∞ as the parameters are all positive. The cost function ϵ is the root-mean-square (RMS) difference between the value of $\Delta\Psi$ predicted by equations (3.6) and (3.27) and the data for each value of (normalised) flow.

The form of the cost function was examined by fixing one of the four parameters and minimising with the other three and plotting the cost against the fixed parameter. Figure 4(a) shows the dependence of the cost function on parameters K_1 and α , and indicates that the parameter K_1 has little effect as long as it is greater than about $K_1 = 5$. For the rest of this paper, K_1 was fixed at a large positive value and not included further in the optimisation. Thus there are three significant parameters: α , K_2 and r_{loss} . Figure 4(b) shows that the parameter α has a significant effect. For the two simulation data

Source	α	K_2	r_{loss} (m Ω)	ϵ (mV)
sim ₀	5.8	1.8×10^{-3}	3.1×10^1	9.2×10^{-3}
sim ₁	5.9	4.6×10^{-3}	4.6×10^1	8.6×10^{-2}
exp	10.9	1.3×10^{-2}	1.0×10^{-6}	1.3
sim ₀	6.0	2.0×10^{-3}	2.7×10^1	5.1×10^{-2}
sim ₁	6.0	4.8×10^{-3}	4.4×10^1	9.0×10^{-2}
exp	6.0	4.4×10^{-3}	5.6×10^1	1.7

Table 2: Optimal parameters. The table summarises the fitting results using the two sets of simulation data (sim₀&sim₁) and the experimental data (exp) from Bazil et al. (2016). Rows 1–3 correspond to free α and the rows 4–6 to fixed $\alpha = 6$.

sets, there is a clear minimum at about $\alpha = 6$. The rows 1–3 of Table 2 show the optimal parameters α , K_2 and r_{loss} , together with the minimal cost ϵ for the two simulations and the experimental data. Rows 4–6 correspond to fixing $\alpha = 6$ and estimating the remaining two parameters K_2 and r_{loss} .

Finally, the current-voltage relationship derived above and given in (3.27) is plotted in Figure 5 for different sets of fitted parameters given in Table 2, along with simulation results from the full model of Bazil et al. (2016), and the corresponding experimental data, showing that the explicit formula for the steady state current/voltage behaviour of the ETC is well captured by the physically plausible model. Figures 5(a)–5(c) correspond to rows 4–6 of Table 2; Figure 5(d) corresponds to row 3 of Table 2.

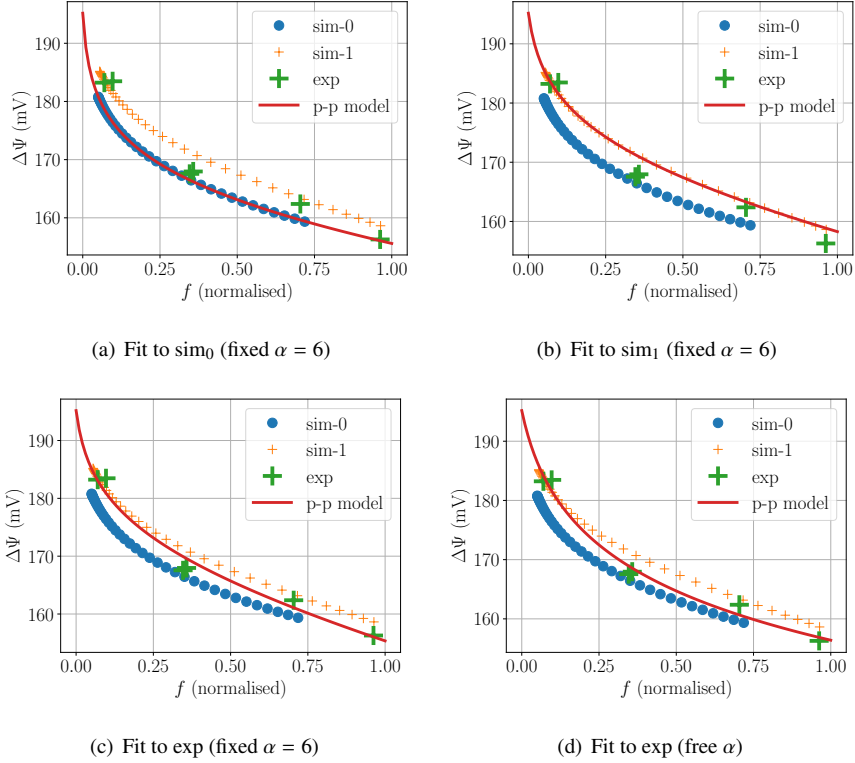


Figure 5: Model fitting. All four plots show four data sets: sim-0 and sim-1 are simulation data from the experimentally fitted simulation of Bazil et al. (2016) for two values of $[\text{Pi}]$; exp is the corresponding experimental data; pp-model is the simulation of the physically-plausible model using the formula of § 3.2. (a) The physically-plausible model is fitted to the experimentally fitted simulation of Bazil et al. (2016) with $[\text{Pi}] = 1 \text{ mM}$ using fixed $\alpha = 6$ and estimating K_2 and r_{loss} . See row 4 of Table 2. (b) As (a) but with $[\text{Pi}] = 5 \text{ mM}$. See row 5 of Table 2. (c) The physically-plausible model is fitted to the experimental points combining both values of Pi using fixed $\alpha = 6$ and estimating K_2 and r_{loss} , see row 6 of Table 2. (d) As (c) except that α is also estimated, see row 3 of Table 2.

4. Discussion

Simplified models of biochemical and biophysical processes have a central role to play in the development of large whole-cell and multi-scale Physiome models, and the use of such models in biomedical and synthetic biology applications. Here we have argued that such simplified models need to be physically plausible, in the sense that they are consistent with the laws of physics (for example, that they obey mass conservation, are consistent with thermodynamic principles, and so on) as well as providing a suitable fit to available data sets. We have demonstrated that energy-based modelling using bond graphs provides a useful framework for the development of such models. The advantages of thermodynamically-consistent modelling have been argued recently by us and a number of other authors (Beard and Qian, 2010; Gawthrop and Crampin, 2014; Klipp et al., 2016; Gawthrop and Crampin, 2017; Mason and Covert, 2019). Key amongst these advantages are that models comprised of physically-plausible components are themselves physically plausible; that such models can be constructed and assembled in a modular fashion; and that such models enforce thermodynamic principles which allow identification of conserved moieties and furthermore restrict the possible parameter space. Here we have shown that by using a modified form of mass action we can generate a simple physically-plausible model of the mitochondrial electron transport chain that is able to reproduce experimentally measured properties of the system.

Bond graphs provide a framework within which is represented both the biochemical network stoichiometry and the constitutive relationship between thermodynamic driving force and biochemical reaction rate for each constituent bond graph element, describing the mechanism of enzymatic processes and so forth. Therefore, bond graphs describe the complete dynamical behaviour of the biochemical system, and can be used to derive the ordinary differential equations describing full system dynamics. A particular advantage, however, of a simple model as derived here over a fully mechanistic model is the possibility of deriving explicit formulae for key properties and behaviours of the system. Here we have shown that using the physically plausible modelling approach we can derive an explicit algebraic formula for the flux through the electron

transport chain to the PMF that is generated across the mitochondrial membrane at steady state, given in equation (3.27). This is not in general possible from a full dynamical representation (whether represented as a bond graph or otherwise). This is of significance both as it drastically simplifies the model, and also because it allows a direct analysis of the dependence of the mitochondrial membrane potential on parameters of the ETC flux, as discussed below. Such a simplified but thermodynamically realistic representation of mitochondrial energy production is particularly suitable to be used in simulation of spatially-distributed networks of mitochondria (Jarosz et al., 2017; Ghosh et al., 2018), for which detailed mechanistic It remains to be determined how different possible modifications to mass action, or indeed other constitutive relations that may be used to relate chemical potential and reaction rate, affect the ability of simple physically plausible models to represent complex biochemical processes. models of mitochondrial bioenergetics have too high a computational overhead.

The physically plausible model of the electron transport chain derived above contains physical parameters which are known *a-priori*, as well as parameters which are model-dependent and therefore obtained by fitting to relevant data. In particular, the explicit formula (3.27) relating flow f to potential difference ΔV has four known physical parameters: ΔV^{eq} , V_N , n_1 and n_2 and four unknown parameters: α , K_1 , K_2 and r_{loss} . Using an optimization approach to model fitting, we have shown that the value of the parameter K_1 appears unimportant, as long as $K_1 > 10$; this corresponds to the rate constant κ_1 of reaction r_1 being large enough so that there is negligible potential drop across the reaction; in other words, this requires that the reaction (3.2) is operating essentially at equilibrium under the experimental conditions considered.

In contrast, the α parameter of the modified mass-action equation (2.21) is found to be important. Choosing $\alpha = 6$ gives a good fit for both the experimentally-fitted simulations and experimental data. This dependence is to be expected as the physically plausible model subsumes a number of individual reactions and this is known to lead to non-stoichiometric exponents (Atkins et al., 2018, chapter 17).

We have shown that despite its simplicity, the physically-plausible model fits the (complex) simulation data from Bazil et al. (2016) closely (RMS error $\epsilon \ll 1$ mV) for both values of Pi and for free α and fixed $\alpha = 6$. Furthermore the experimental data

can be fitted with the model with an error ϵ of about 2 mV.

Despite the success of the simplified, physically-plausible model of the electron transport chain that we have developed here, it should be noted that there are choices and trade-offs inherent in the simplification process. Therefore it is important that such simplified models are analysed and used only in the appropriate context. Firstly, the simplified model was generated using a specific form of modified mass action kinetics. While motivated by existing literature and approaches for representing non-elemental biochemical reaction steps, different choices could have been made. It remains to be determined how different possible modifications to mass action, or indeed other constitutive relations that may be used to relate chemical potential and reaction rate, affect the ability of simple physically plausible models to represent complex biochemical processes.

Secondly, the simplified model was developed using data relevant to normal physiological conditions. Most significantly, simplifying assumptions have been made about the physiological regime in which the model operates, and hence perturbations to species concentrations and specific enzymatic regulators outside of this regime are not captured in the simplified model. Full mechanistic exploration of mitochondrial dynamics under a broad range of perturbations and experimental data beyond those used to fit the simplified model should of course be pursued using the full bond graph representation of mitochondrial bioenergetics.

Finally, because the physically-plausible model is energy based, any or all of the **Ce** components can provide connections with energy-based models of other parts of the mitochondria system such as the TCA cycle, ATPase and ROS generation. In bond graph terminology, the **Ce** components become *ports* (Gawthrop and Crampin, 2018b) with which to connect to other bond graph components representing other aspects of mitochondrial biochemistry, for simulation and analysis of larger-scale models of mitochondrial and cellular bioenergetics. In our future work we intend to exploit this feature of bond graphs to investigate in larger models of mitochondrial function the basis of ROS generation and damage.

Acknowledgements

PJG would like to thank the Melbourne School of Engineering for its support via a Professorial Fellowship. This research was in part conducted and funded by the Australian Research Council Centre of Excellence in Convergent Bio-Nano Science and Technology (project number CE140100036). The authors would like to thank an anonymous reviewer for pointing out an error in an early version of the manuscript and suggesting a number of points of clarification.

References

- Peter Atkins, Julio De Paula, and James Keeler. *Atkins' Physical Chemistry*. Oxford University Press, Oxford, 11th edition, 2018.
- Jason N. Bazil, Daniel A. Beard, and Kalyan C. Vinnakota. Catalytic coupling of oxidative phosphorylation, ATP demand, and reactive oxygen species generation. *Biophysical Journal*, 110(4):962 – 971, 2016. ISSN 0006-3495. doi:10.1016/j.bpj.2015.09.036.
- Daniel A Beard. A biophysical model of the mitochondrial respiratory system and oxidative phosphorylation. *PLoS Comput Biol*, 1(4):e36, 09 2005. doi:10.1371/journal.pcbi.0010036.
- Daniel A. Beard. *Biosimulation: Simulation of Living Systems*. Cambridge University Press, Cambridge, UK., 2012. ISBN 978-0-521-76823-8.
- Daniel A Beard and Hong Qian. *Chemical biophysics: quantitative analysis of cellular systems*. Cambridge University Press, 2010.
- Wolfgang Borutzky. *Bond graph methodology: development and analysis of multidisciplinary dynamic system models*. Springer, Berlin, 2010. ISBN 978-1-84882-881-0. doi:10.1007/978-1-84882-882-7.
- F.J. Bruggeman, J.L. Snoep, and H.V. Westerhoff. Control, responses and modularity of cellular regulatory networks: a control analysis perspective. *Systems Biology, IET*, 2(6):397–410, November 2008. ISSN 1751-8849. doi:10.1049/iet-syb:20070065.

- Frank J. Bruggeman, Hans V. Westerhoff, Jan B. Hoek, and Boris N. Kholodenko. Modular response analysis of cellular regulatory networks. *Journal of Theoretical Biology*, 218(4):507 – 520, 2002. ISSN 0022-5193. doi:10.1006/jtbi.2002.3096.
- F. E. Cellier. *Continuous system modelling*. Springer-Verlag, New York, 1991.
- E. J. Crampin, N. P. Smith, and P. J. Hunter. Multi-scale modelling and the IUPS Physiome project. *Journal of Molecular Histology*, 35(7):707–714, 2004.
- Marie E. Csete and John C. Doyle. Reverse engineering of biological complexity. *Science*, 295(5560):1664–1669, 2002. doi:10.1126/science.1069981.
- Peter Cudmore, Peter J. Gawthrop, Michael Pan, and Edmund J. Crampin. Computer-aided modelling of complex physical systems with BondGraphTools. Jun 2019.
- Alexander P. S. Darlington, Juhyun Kim, Jose I. Jimenez, and Declan G. Bates. Dynamic allocation of orthogonal ribosomes facilitates uncoupling of co-expressed genes. *Nature Communications*, 9(1):695, 2018. ISSN 2041-1723. doi:10.1038/s41467-018-02898-6.
- Domitilla Del Vecchio. A control theoretic framework for modular analysis and design of biomolecular networks. *Annual Reviews in Control*, 37(2):333 – 345, 2013. ISSN 1367-5788. doi:10.1016/j.arcontrol.2013.09.011.
- Domitilla Del Vecchio and Richard M Murray. *Biomolecular Feedback Systems*. Princeton University Press, 2014. ISBN 0691161534.
- P. Gawthrop and E. J. Crampin. Bond graph representation of chemical reaction networks. *IEEE Transactions on NanoBioscience*, 17(4):449–455, October 2018a. ISSN 1536-1241. doi:10.1109/TNB.2018.2876391. Available at arXiv:1809.00449.
- P. J. Gawthrop. Bond graph modeling of chemiosmotic biomolecular energy transduction. *IEEE Transactions on NanoBioscience*, 16(3):177–188, April 2017. ISSN 1536-1241. doi:10.1109/TNB.2017.2674683. Available at arXiv:1611.04264.

- P. J. Gawthrop and E. J. Crampin. Modular bond-graph modelling and analysis of biomolecular systems. *IET Systems Biology*, 10(5):187–201, October 2016. ISSN 1751-8849. doi:10.1049/iet-syb.2015.0083. Available at arXiv:1511.06482.
- P. J. Gawthrop and L. P. S. Smith. *Metamodelling: Bond Graphs and Dynamic Systems*. Prentice Hall, Hemel Hempstead, Herts, England., 1996. ISBN 0-13-489824-9.
- P. J. Gawthrop, I. Siekmann, T. Kameneva, S. Saha, M. R. Ibbotson, and E. J. Crampin. Bond graph modelling of chemoelectrical energy transduction. *IET Systems Biology*, 11(5):127–138, 2017. ISSN 1751-8849. doi:10.1049/iet-syb.2017.0006. Available at arXiv:1512.00956.
- Peter J Gawthrop. Physically-plausible models for identification. In *Proceedings of the 2003 International Conference On Bond Graph Modeling and Simulation (ICBGM'03)*, Simulation Series, pages 59–64, Orlando, Florida, U.S.A., January 2003. Society for Computer Simulation.
- Peter J Gawthrop and Geraint P Bevan. Bond-graph modeling: A tutorial introduction for control engineers. *IEEE Control Systems Magazine*, 27(2):24–45, April 2007. doi:10.1109/MCS.2007.338279.
- Peter J. Gawthrop and Edmund J. Crampin. Energy-based analysis of biochemical cycles using bond graphs. *Proceedings of the Royal Society A: Mathematical, Physical and Engineering Science*, 470(2171):1–25, 2014. doi:10.1098/rspa.2014.0459. Available at arXiv:1406.2447.
- Peter J. Gawthrop and Edmund J. Crampin. Energy-based analysis of biomolecular pathways. *Proceedings of the Royal Society of London A: Mathematical, Physical and Engineering Sciences*, 473(2202), 2017. ISSN 1364-5021. doi:10.1098/rspa.2016.0825. Available at arXiv:1611.02332.
- Peter J. Gawthrop and Edmund J. Crampin. Biomolecular system energetics. In *Proceedings of the 13th International Conference on Bond Graph Modeling (ICBGM'18)*, Bordeaux, 2018b. Society for Computer Simulation. Available at arXiv:1803.09231.

- Peter J. Gawthrop, Joseph Cursons, and Edmund J. Crampin. Hierarchical bond graph modelling of biochemical networks. *Proceedings of the Royal Society A: Mathematical, Physical and Engineering Sciences*, 471(2184):1–23, 2015. ISSN 1364-5021. doi:10.1098/rspa.2015.0642. Available at arXiv:1503.01814.
- Shouryadipta Ghosh, Kenneth Tran, Edmund Crampin, Eric Hanssen, and Vijay Rajagopal. Creatine-kinase shuttle and rapid mitochondrial membrane potential conductivity are needed simultaneously to maintain uniform metabolite distributions in the cardiac cell contraction cycle. *Biophysical Journal*, 114(3, Supplement 1):550a, 2018. ISSN 0006-3495. doi:10.1016/j.bpj.2017.11.3004.
- Leland H Hartwell, John J Hopfield, Stanislas Leibler, and Andrew W Murray. From molecular to modular cell biology. *Nature*, 402:C47–C52, 1999.
- Peter Hunter. The virtual physiological human: The physiome project aims to develop reproducible, multiscale models for clinical practice. *IEEE Pulse*, 7(4):36–42, July 2016. ISSN 2154-2287. doi:10.1109/MPUL.2016.2563841.
- Jan Jarosz, Shouryadipta Ghosh, Lea M. D. Delbridge, Amorita Petzer, Anthony J. R. Hickey, Edmund J. Crampin, Eric Hanssen, and Vijay Rajagopal. Changes in mitochondrial morphology and organization can enhance energy supply from mitochondrial oxidative phosphorylation in diabetic cardiomyopathy. *American Journal of Physiology - Cell Physiology*, 312(2):C190–C197, 2017. ISSN 0363-6143. doi:10.1152/ajpcell.00298.2016.
- S. Jayanthi and Domitilla Del Vecchio. Retroactivity attenuation in bio-molecular systems based on timescale separation. *Automatic Control, IEEE Transactions on*, 56(4):748–761, April 2011. ISSN 0018-9286. doi:10.1109/TAC.2010.2069631.
- Dean C Karnopp, Donald L Margolis, and Ronald C Rosenberg. *System Dynamics: Modeling, Simulation, and Control of Mechatronic Systems*. John Wiley & Sons, 5th edition, 2012. ISBN 978-0470889084.
- Jonathan R. Karr, Jayodita C. Sanghvi, Derek N. Macklin, Miriam V. Gutschow, Jared M. Jacobs, Benjamin Bolival Jr., Nacyra Assad-Garcia, John I. Glass,

- and Markus W. Covert. A whole-cell computational model predicts phenotype from genotype. *Cell*, 150(2):389 – 401, 2012. ISSN 0092-8674. doi:10.1016/j.cell.2012.05.044.
- Edda Klipp, Wolfram Liebermeister, Christoph Wierling, and Axel Kowald. *Systems biology: a textbook*. Wiley-VCH, Weinheim, Germany, 2nd edition, 2016.
- Douglas A. Lauffenburger. Cell signaling pathways as control modules: Complexity for simplicity? *Proceedings of the National Academy of Sciences*, 97(10):5031–5033, 2000. doi:10.1073/pnas.97.10.5031.
- Derek N Macklin, Nicholas A Ruggero, and Markus W Covert. The future of whole-cell modeling. *Current Opinion in Biotechnology*, 28(0):111 – 115, 2014. ISSN 0958-1669. doi:10.1016/j.copbio.2014.01.012.
- John C. Mason and Markus W. Covert. An energetic reformulation of kinetic rate laws enables scalable parameter estimation for biochemical networks. *Journal of Theoretical Biology*, 461:145 – 156, 2019. ISSN 0022-5193. doi:<https://doi.org/10.1016/j.jtbi.2018.10.041>. URL <http://www.sciencedirect.com/science/article/pii/S002251931830523X>.
- Peter Mitchell. Coupling of phosphorylation to electron and hydrogen transfer by a chemi-osmotic type of mechanism. *Nature*, 191(4784):144–148, Jul 1961. doi:10.1038/191144a0.
- Peter Mitchell. Possible molecular mechanisms of the protonmotive function of cytochrome systems. *Journal of Theoretical Biology*, 62(2):327–367, 1976. doi:10.1016/0022-5193(76)90124-7.
- Peter Mitchell. David Keilin’s Respiratory Chain Concept and its Chemiosmotic Consequences. In Tore Frängsmyr and Sture Forsén, editors, *Nobel Lectures in Chemistry, 1971-1980*. World Scientific, Singapore, 1993. ISBN 981-02-0786-7.
- Peter Mitchell. Chemiosmotic coupling in oxidative and photosynthetic phosphorylation. *Biochimica et Biophysica Acta (BBA) - Bioenergetics*, 1807(12):1507 – 1538,

2011. ISSN 0005-2728. doi:10.1016/j.bbablo.2011.09.018. Special Section: Peter Mitchell - 50th anniversary of the chemiosmotic theory.
- Michael P. Murphy. How mitochondria produce reactive oxygen species. *Biochemical Journal*, 417(1):1–13, 2009. ISSN 0264-6021. doi:10.1042/BJ20081386.
- Maxwell L. Neal, Michael T. Cooling, Lucian P. Smith, Christopher T. Thompson, Herbert M. Sauro, Brian E. Carlson, Daniel L. Cook, and John H. Gennari. A reappraisal of how to build modular, reusable models of biological systems. *PLoS Comput Biol*, 10(10):e1003849, 10 2014. doi:10.1371/journal.pcbi.1003849.
- David G Nicholls and Stuart Ferguson. *Bioenergetics 4*. Academic Press, Amsterdam, 2013.
- David Nickerson, Koray Atalag, Bernard de Bono, Jörg Geiger, Carole Goble, Susanne Hollmann, Joachim Lonien, Wolfgang Müller, Babette Regierer, Natalie J. Stanford, Martin Golebiewski, and Peter Hunter. The human physiome: how standards, software and innovative service infrastructures are providing the building blocks to make it achievable. *Interface Focus*, 6(2), 2016. ISSN 2042-8898. doi:10.1098/rsfs.2015.0103.
- George Oster, Alan Perelson, and Aharon Katchalsky. Network thermodynamics. *Nature*, 234:393–399, December 1971. doi:10.1038/234393a0.
- George F. Oster, Alan S. Perelson, and Aharon Katchalsky. Network thermodynamics: dynamic modelling of biophysical systems. *Quarterly Reviews of Biophysics*, 6(01): 1–134, 1973. doi:10.1017/S0033583500000081.
- Bernhard Palsson. *Systems biology: properties of reconstructed networks*. Cambridge University Press, 2006. ISBN 0521859034.
- Bernhard Palsson. *Systems Biology: Simulation of Dynamic Network States*. Cambridge University Press, 2011.
- Bernhard Palsson. *Systems Biology: Constraint-Based Reconstruction and Analysis*. Cambridge University Press, Cambridge, 2015.

- Michael Pan, Peter J. Gawthrop, Kenneth Tran, Joseph Cursons, and Edmund J. Crampin. Bond graph modelling of the cardiac action potential: implications for drift and non-unique steady states. *Proceedings of the Royal Society of London A: Mathematical, Physical and Engineering Sciences*, 474(2214), 2018. ISSN 1364-5021. doi:10.1098/rspa.2018.0106. Available at arXiv:1802.04548.
- Michael Pan, Peter J. Gawthrop, Kenneth Tran, Joseph Cursons, and Edmund J. Crampin. A thermodynamic framework for modelling membrane transporters. *Journal of Theoretical Biology*, 481:10 – 23, 2019. ISSN 0022-5193. doi:10.1016/j.jtbi.2018.09.034. Available at arXiv:1806.04341.
- H. M. Paynter. *Analysis and design of engineering systems*. MIT Press, Cambridge, Mass., 1961.
- Jan Willem Polderman and Jan C. Willems. *Introduction to Mathematical System Theory: A Behavioral Approach*. Number 26 in Texts in Applied Mathematics. Springer, 1997.
- Matteo Poletti and Massimiliano Esposito. Irreversible thermodynamics of open chemical networks. I. Emergent cycles and broken conservation laws. *The Journal of Chemical Physics*, 141(2):024117, 2014. doi:10.1063/1.4886396.
- Anna Maria Porcelli, Anna Ghelli, Claudia Zanna, Paolo Pinton, Rosario Rizzuto, and Michela Rugolo. pH difference across the outer mitochondrial membrane measured with a green fluorescent protein mutant. *Biochemical and Biophysical Research Communications*, 326(4):799 – 804, 2005. ISSN 0006-291X. doi:10.1016/j.bbrc.2004.11.105.
- Matthew Scott, Stefan Klumpp, Eduard M Mateescu, and Terence Hwa. Emergence of robust growth laws from optimal regulation of ribosome synthesis. *Molecular Systems Biology*, 10(8):747, 2014. doi:10.15252/msb.20145379.
- Z. Szallasi, V. Periwal, and Jorg Stelling. On modules and modularity. In Z. Szallasi, J. Stelling, and V. Periwal, editors, *System Modeling in Cellular Biology: From Concepts to Nuts and Bolts*, pages 19–40. MIT press, 2010.

- Andrea Y. Weiße, Diego A. Oyarzún, Vincent Danos, and Peter S. Swain. Mechanistic links between cellular trade-offs, gene expression, and growth. *Proceedings of the National Academy of Sciences*, 112(9):E1038–E1047, 2015. ISSN 0027-8424. doi:10.1073/pnas.1416533112.
- J. C. Willems. Dissipative dynamical systems, part I: General theory, part II: Linear system with quadratic supply rates. *Arch. Rational Mechanics and Analysis*, 45(5): 321–392, 1972.
- J. C. Willems. The behavioral approach to open and interconnected systems. *IEEE Control Systems*, 27(6):46–99, Dec 2007. ISSN 1066-033X. doi:10.1109/MCS.2007.906923.
- Fan Wu, Feng Yang, Kalyan C. Vinnakota, and Daniel A. Beard. Computer modeling of mitochondrial tricarboxylic acid cycle, oxidative phosphorylation, metabolite transport, and electrophysiology. *Journal of Biological Chemistry*, 282(34):24525–24537, 2007. doi:10.1074/jbc.M701024200.